

## Article

# Magnetic Properties of the $\text{Mn}_{55}\text{Bi}_{45}/\text{Nd}_2\text{Fe}_{14}\text{B}$ Hybrid Magnetic Alloys

Shunda Lu, Yang Yang, Linfeng Chen, Zhen Xiang \* and Wei Lu \*

Shanghai Key Laboratory of D&amp;A for Metal-Functional Materials, School of Materials Science &amp; Engineering, Tongji University, Shanghai 201804, China

\* Correspondence: xiangzhen@tongji.edu.cn (Z.X.); weilu@tongji.edu.cn (W.L.)

**Abstract:** The  $(\text{Mn}_{55}\text{Bi}_{45})_{100-x}/(\text{Nd}_2\text{Fe}_{14}\text{B})_x$  hybrid magnetic alloys were prepared by the ball milling of the combined annealed  $\text{Mn}_{55}\text{Bi}_{45}$  powders and  $\text{Nd}_2\text{Fe}_{14}\text{B}$  powders. The magnetic properties at room temperature and elevated temperature were investigated. It was found that the saturation magnetization and the coercivity at room temperature increased significantly with the increasing  $\text{Nd}_2\text{Fe}_{14}\text{B}$  content. The enhanced energy product of 10.8 MGOe and 11.5 MGOe were obtained in  $(\text{Mn}_{55}\text{Bi}_{45})_{40}/(\text{Nd}_2\text{Fe}_{14}\text{B})_{60}$  and  $(\text{Mn}_{55}\text{Bi}_{45})_{20}/(\text{Nd}_2\text{Fe}_{14}\text{B})_{80}$ . At elevated temperatures (350 K), the coercivities of 16.6 kOe and 16.1 kOe were obtained with  $\text{Nd}_2\text{Fe}_{14}\text{B}$  content of 20 wt.% and 40 wt.%, which were higher than those at room temperature. The temperature coefficients of coercivity of  $(\text{Mn}_{55}\text{Bi}_{45})_{80}/(\text{Nd}_2\text{Fe}_{14}\text{B})_{20}$  and  $(\text{Mn}_{55}\text{Bi}_{45})_{60}/(\text{Nd}_2\text{Fe}_{14}\text{B})_{40}$  were calculated to be positive, owing to the coercivity temperature characteristics of MnBi alloy. Finally, the energy products remained 10.5 MGOe and 10.1 MGOe in  $(\text{Mn}_{55}\text{Bi}_{45})_{40}/(\text{Nd}_2\text{Fe}_{14}\text{B})_{60}$  and  $(\text{Mn}_{55}\text{Bi}_{45})_{20}/(\text{Nd}_2\text{Fe}_{14}\text{B})_{80}$  at 350 K, which exhibited potential for high temperature applications.

**Keywords:** MnBi alloy; NdFeB alloy; hybrid magnetic alloys; magnetic properties



**Citation:** Lu, S.; Yang, Y.; Chen, L.; Xiang, Z.; Lu, W. Magnetic Properties of the  $\text{Mn}_{55}\text{Bi}_{45}/\text{Nd}_2\text{Fe}_{14}\text{B}$  Hybrid Magnetic Alloys. *Metals* **2022**, *12*, 1543. <https://doi.org/10.3390/met12091543>

Academic Editors: Jiro Kitagawa and Imre Bakonyi

Received: 28 June 2022

Accepted: 31 August 2022

Published: 19 September 2022

**Publisher's Note:** MDPI stays neutral with regard to jurisdictional claims in published maps and institutional affiliations.



**Copyright:** © 2022 by the authors. Licensee MDPI, Basel, Switzerland. This article is an open access article distributed under the terms and conditions of the Creative Commons Attribution (CC BY) license (<https://creativecommons.org/licenses/by/4.0/>).

## 1. Introduction

Permanent magnet materials are key materials in the production of electronics, synchronous motors, electric vehicles and wind power generators [1–3]. MnBi alloys have attracted extensive attention due to their unique magnetic properties, such as a theoretical maximum energy product of 17.6 MGOe [4], a large magnetocrystalline anisotropy energy of 1.6 MJ/m<sup>3</sup> at room temperature [5,6], a high Curie temperature of 711 K [7], and, especially, the positive temperature coefficient of coercivity [8–10], which make the MnBi alloy a promising candidate for high temperature applications.

The low temperature phase MnBi (LTP-MnBi) with a NiAs-type hexagonal structure is formed by peritectic reaction at 628 K [11,12]. During the solidification process, the Mn element can be easily segregated and oxidized, which hinders the formation of LTP-MnBi and damages magnetic properties directly. Gabay [13] produced an MnBi alloy ribbon with a high purity LTP content of 98 wt.% by melting and spinning, followed by an annealing process. The results demonstrated that a smaller ejection orifice led to a higher saturation magnetization. Finally, a high saturation magnetization value of 78 emu/g was obtained. Xiang [14] prepared MnBi powder by induction melting, followed by annealing and low energy ball milling. The ball milling process reduced MnBi particle size to 0.7 μm. The saturation magnetization decreased due to the decomposition of LTP-MnBi during the milling process, but the coercivity increased to 1.9 T.

Furthermore, element doping is considered to be an effective way to regulate the magnetic properties of MnBi alloys. Dopant atoms can occupy the lattice positions or enter interstitial sites to optimum lattice parameters, especially the *c/a* ratio, which was closely related to the magnetocrystalline anisotropy [4,15–18]. Yang [19] investigated the effect of Ga-doping on the magnetic properties of MnBi alloys. The results showed that

the coercivity enhanced with the increase of Ga content. A high coercivity of 1.66 T and an energy product of 7.87 MGOe were obtained. Bae [20] fabricated Sb-doped MnBi alloys and found that an appropriate addition of Sb element was able to refine the grain size of MnBi particles. The saturation magnetization, coercivity, and the maximum energy product were 64.7 emu/g, 1.5 T, and 11.0 MGOe, respectively, in  $\text{Mn}_{54}\text{Bi}_{45.9}\text{Sb}_{0.1}$  ball-milled powder. In addition to element doping, Xu [21] successfully synthesized the exchange coupled hard/soft MnBi/Fe-Co composite powders by using a magnetic self-assembly process. An enhanced remanence magnetization was obtained, owing to the high magnetization of Fe-Co nanoparticles. Yang [22] prepared the anisotropic MnBi/ $\text{Sm}_2\text{Fe}_{17}\text{N}_x$  hybrid magnet by the grinding of high purity MnBi ribbons and  $\text{Sm}_2\text{Fe}_{17}\text{N}_x$  particles together. The strong exchange coupling effect between MnBi and  $\text{Sm}_2\text{Fe}_{17}\text{N}_x$  led to both high remanence and high coercivity from 250 K to 380 K. The maximum energy products of 18 MGOe at 300 K, and 10 MGOe at 380 K were obtained. Therefore, it was found that the hybridization of MnBi alloys with other hard/soft magnetic materials is beneficial to compensate respective disadvantages and reach high magnetic properties. It is well-known that NdFeB alloys have been used in many fields due to its excellent magnetic properties at room temperature. However, the negative temperature coefficient of coercivity and low Curie temperature (583 K) restrict the further development of NdFeB alloys in the field of high temperatures [23].

In this work, the bulk  $(\text{Mn}_{55}\text{Bi}_{45})_{100-x}/(\text{Nd}_2\text{Fe}_{14}\text{B})_x$  hybrid magnetic alloys are prepared by the ball milling of  $\text{Mn}_{55}\text{Bi}_{45}$  powder and  $\text{Nd}_2\text{Fe}_{14}\text{B}$  powder together, followed by a cold press process. The magnetic properties at room temperature and elevated temperature were investigated. Due to the excellent room temperature the magnetic properties of NdFeB alloy and the positive temperature coefficient of coercivity of MnBi alloy, the hybrid magnetic alloys will exhibit good magnetic properties at room temperature and elevated temperature, which is favorable for applications in various fields.

## 2. Materials and Methods

The  $\text{Mn}_{55}\text{Bi}_{45}$  alloy ingot was prepared by induction melting with high purity (99.99%) Mn and Bi elements under high purity argon atmosphere. Excess 5 wt.% Mn was added to compensate for the evaporation loss of Mn during the melting process. The obtained ingot was annealed at 290 °C for 12 h in a high vacuum ( $10^{-5}$  Pa) with a tube furnace and then cooled with the furnace. The annealed ingot was crushed and ground into powders in ethanol by using a pestle and mortar. The powders were vacuum dried and then sieved using #300 mesh to ensure the particle sizes were less than 48  $\mu\text{m}$ . Then, the  $\text{Mn}_{55}\text{Bi}_{45}$  powders were mixed with  $\text{Nd}_2\text{Fe}_{14}\text{B}$  powders according to different weight percentages to prepared  $(\text{Mn}_{55}\text{Bi}_{45})_{100-x}/(\text{Nd}_2\text{Fe}_{14}\text{B})_x$  ( $x = 0, 20, 40, 60, 80,$  and  $100$ ) hybrid permanent magnetic powders. The  $(\text{Mn}_{55}\text{Bi}_{45})_{100-x}/(\text{Nd}_2\text{Fe}_{14}\text{B})_x$  hybrid powders were ball milled for 2 h with a milling speed of 100 r/min at room temperature. The ball milling process was carried out with zirconia balls (3 mm in diameter) in 100 mL zirconia jars. The ball milling medium was ethanol, and the ball-to-powder weight ratio was about 10:1. Finally, 10 g of  $(\text{Mn}_{55}\text{Bi}_{45})_{100-x}/(\text{Nd}_2\text{Fe}_{14}\text{B})_x$  hybrid magnetic powders were taken to be cold pressed under a pressure of 400 MPa at room temperature. The cold press process was carried out under vacuum ( $10^{-3}$  Pa) by using a hard alloy mold with a diameter of 10 mm. The cold-pressed sample was a cylinder with a diameter of 10 mm and a height of 4 mm. Blocks with a size of 2 mm  $\times$  2 mm  $\times$  2 mm were cut from the cold-pressed sample and were magnetically orientated under a pulsed magnetic field of 18 kOe.

The crystallographic structure of the hybrid magnetic powders was identified by X-ray diffraction (XRD) with  $\text{Cu-K}_\alpha$  ( $\lambda = 1.5406 \text{ \AA}$ ) radiation. The densities of the cold-pressed bulk samples were measured by the Archimedes method. The magnetic properties were characterized under an applied field of 30 kOe by using a Physical Property Measurement System (PPMS) equipped with a Vibrating Sample Magnetometer (VSM).

### 3. Results and Discussion

#### 3.1. Microstructure of $Mn_{55}Bi_{45}/Nd_2Fe_{14}B$ Hybrid Magnetic Alloys

Figure 1 showed the typical XRD patterns of  $(Mn_{55}Bi_{45})_{100-x}/(Nd_2Fe_{14}B)_x$  hybrid magnetic powders after ball milling process. It was observed that the pure  $Mn_{55}Bi_{45}$  ( $x = 0$ ) powders consisted of a high purity LTP-MnBi (>90 wt.%) and a small amount of Bi phase and Mn phase. With the increase of  $Nd_2Fe_{14}B$  content, the diffraction peak intensity of  $Nd_2Fe_{14}B$  phase gradually increased. It was clearly seen that the diffraction peaks of LTP-MnBi and  $Nd_2Fe_{14}B$  phase existed simultaneously, which indicated that the  $Mn_{55}Bi_{45}$  powder was well mixed with the  $Nd_2Fe_{14}B$  powder. Figure 2 showed the densities of the bulk  $(Mn_{55}Bi_{45})_{100-x}/(Nd_2Fe_{14}B)_x$  hybrid magnetic alloys with different  $Nd_2Fe_{14}B$  content. The density values were illustrated in Table 1. For the pure  $Mn_{55}Bi_{45}$  ( $x = 0$ ), a density value of  $8.61 \text{ g/cm}^3$  was obtained, which reached 96.7% of the theoretical density value ( $8.9 \text{ g/cm}^3$ ) of MnBi alloy. With the increase of the  $Nd_2Fe_{14}B$  content, the density values of the bulk hybrid magnetic alloys gradually decreased, which was due to the relatively low density value of the  $Nd_2Fe_{14}B$  alloy ( $7.45 \text{ g/cm}^3$ ).

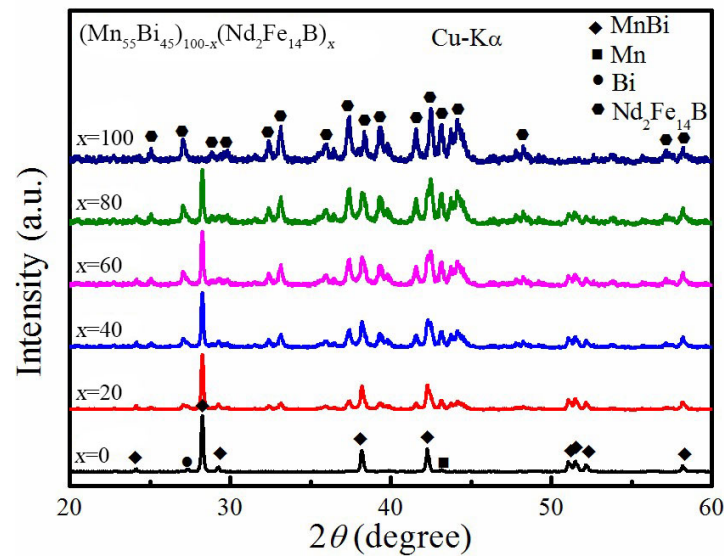


**Figure 1.** The XRD patterns of  $(Mn_{55}Bi_{45})_{100-x}/(Nd_2Fe_{14}B)_x$  ( $x = 0, 20, 40, 60, 80,$  and  $100$ ) hybrid magnetic powders.

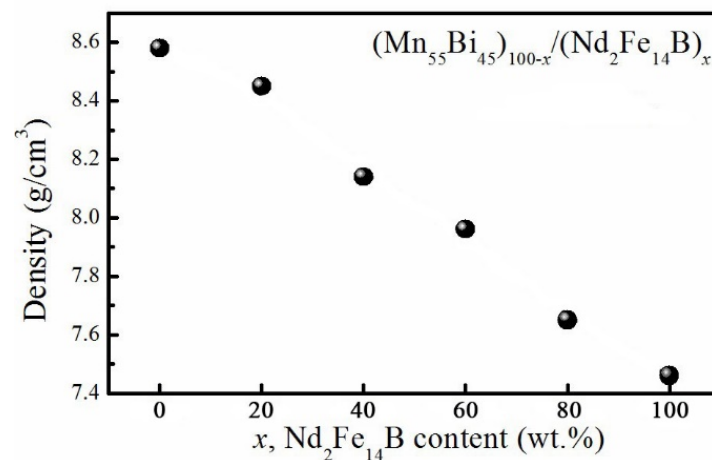


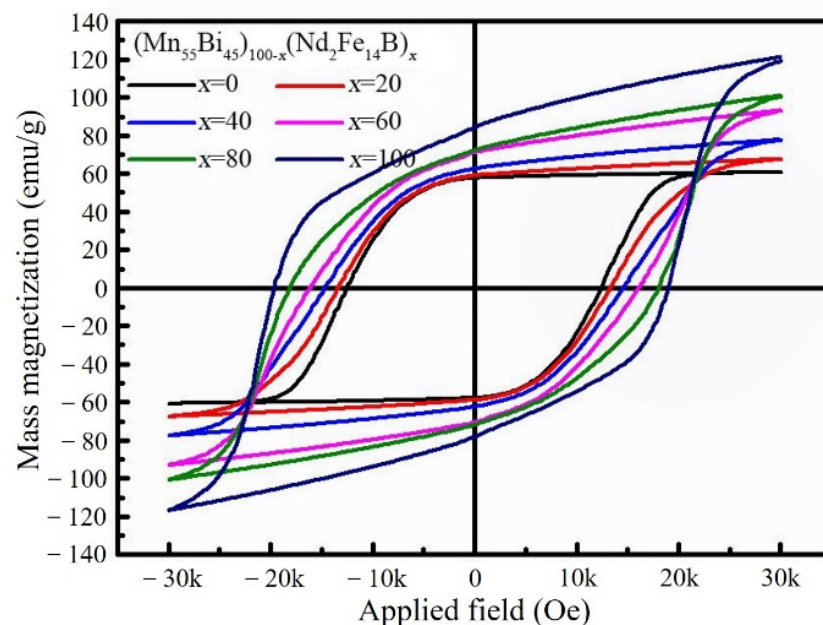
**Figure 2.** The densities of the bulk  $(Mn_{55}Bi_{45})_{100-x}/(Nd_2Fe_{14}B)_x$  ( $x = 0, 20, 40, 60, 80,$  and  $100$ ) hybrid magnetic alloys.

**Table 1.** The density values of the bulk  $(\text{Mn}_{55}\text{Bi}_{45})_{100-x}/(\text{Nd}_2\text{Fe}_{14}\text{B})_x$  hybrid magnetic alloys.

$(\text{Mn}_{55}\text{Bi}_{45})_{100-x}/(\text{Nd}_2\text{Fe}_{14}\text{B})_x$	Density ( $\text{g}/\text{cm}^3$ )
$x = 0$	$8.61 \pm 0.02$
$x = 20$	$8.45 \pm 0.03$
$x = 40$	$8.14 \pm 0.02$
$x = 60$	$7.96 \pm 0.03$
$x = 80$	$7.66 \pm 0.04$
$x = 100$	$7.45 \pm 0.02$

### 3.2. The Magnetic Properties of $\text{Mn}_{55}\text{Bi}_{45}/\text{Nd}_2\text{Fe}_{14}\text{B}$ Hybrid Magnetic Alloys at Room Temperature

Figure 3 showed the room temperature hysteresis loops of the bulk  $(\text{Mn}_{55}\text{Bi}_{45})_{100-x}/(\text{Nd}_2\text{Fe}_{14}\text{B})_x$  hybrid magnetic alloys. No obvious kinks were observed for all the loops, indicating good exchange coupling between grains of these two phases. The pure  $\text{Mn}_{55}\text{Bi}_{45}$  featured with a great  $M_r/M_s$  value, which indicated an magnetocrystalline anisotropy along with  $c$ -axis. With the increase of  $\text{Nd}_2\text{Fe}_{14}\text{B}$  content, the  $M_r/M_s$  values gradually decreased. Figure 4 and Table 2 show the variations of saturation magnetization ( $M_s$ ), coercivity ( $H_c$ ), and maximum energy product  $(BH)_{\max}$  with the increasing  $\text{Nd}_2\text{Fe}_{14}\text{B}$  content. For the pure  $\text{Mn}_{55}\text{Bi}_{45}$  ( $x = 0$ ), a  $M_s$  of 61.2 emu/g, a  $H_c$  of 12.5 kOe, and a  $(BH)_{\max}$  of 9.8 MGOe were obtained. With the increase of  $\text{Nd}_2\text{Fe}_{14}\text{B}$  content, both the  $M_s$  and  $H_c$  of the bulk  $(\text{Mn}_{55}\text{Bi}_{45})_{100-x}/(\text{Nd}_2\text{Fe}_{14}\text{B})_x$  hybrid magnetic alloys were significantly enhanced, mainly owing to the excellent magnetic properties ( $M_s = 120.9$  emu/g,  $H_c = 19.7$  kOe) of  $\text{Nd}_2\text{Fe}_{14}\text{B}$  alloy at room temperature. However, it was noted that the  $(BH)_{\max}$  of the hybrid magnetic alloys decreased when  $\text{Nd}_2\text{Fe}_{14}\text{B}$  content was 20 wt.% and 40 wt.%. The decrease in  $(BH)_{\max}$  was mainly caused by the declined densities. When  $\text{Nd}_2\text{Fe}_{14}\text{B}$  content further increased to 60 wt.% and 80 wt.%, the  $(BH)_{\max}$  enhanced to 10.8 MGOe and 11.5 MGOe, which indicated 10% and 17% increase compared to  $\text{Mn}_{55}\text{Bi}_{45}$ , respectively. Therefore, it was demonstrated that the addition of  $\text{Nd}_2\text{Fe}_{14}\text{B}$  alloy can improve the room temperature magnetic properties of MnBi alloy.

**Figure 3.** The room temperature hysteresis loops of the bulk  $(\text{Mn}_{55}\text{Bi}_{45})_{100-x}/(\text{Nd}_2\text{Fe}_{14}\text{B})_x$  ( $x = 0, 20, 40, 60, 80,$  and  $100$ ) hybrid magnetic alloys.

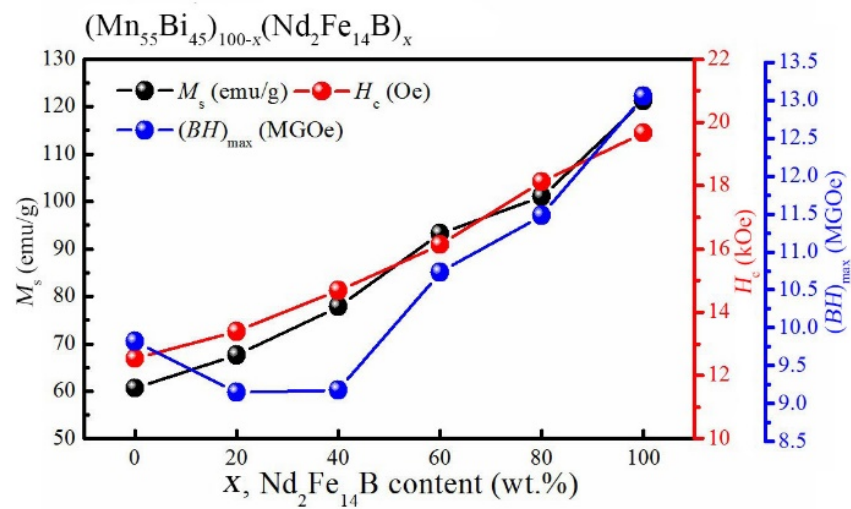


**Figure 4.** The variation curves of saturation magnetization ( $M_s$ ), coercivity ( $H_c$ ), and maximum energy product  $(BH)_{\max}$  of the bulk  $(\text{Mn}_{55}\text{Bi}_{45})_{100-x}/(\text{Nd}_2\text{Fe}_{14}\text{B})_x$  ( $x = 0, 20, 40, 60, 80,$  and  $100$ ) hybrid magnetic alloys with the increase of  $\text{Nd}_2\text{Fe}_{14}\text{B}$  content.

**Table 2.** The room temperature magnetic properties of the bulk  $(\text{Mn}_{55}\text{Bi}_{45})_{100-x}/(\text{Nd}_2\text{Fe}_{14}\text{B})_x$  hybrid magnetic alloys.

$(\text{Mn}_{55}\text{Bi}_{45})_{100-x}/(\text{Nd}_2\text{Fe}_{14}\text{B})_x$	$M_s$ (emu/g)	$H_c$ (kOe)	$(BH)_{\max}$ (MGOe)	$M_r/M_s$
$x = 0$	61.2 (4)	12.5 (3)	9.8 (2)	0.98
$x = 20$	67.6 (2)	13.4 (2)	9.1 (6)	0.89
$x = 40$	78.2 (1)	14.8 (7)	9.2 (1)	0.80
$x = 60$	93.8 (6)	16.2 (4)	10.7 (6)	0.76
$x = 80$	101.4 (5)	18.1 (8)	11.5 (1)	0.71
$x = 100$	120.9 (2)	19.7 (2)	13.0 (9)	0.69

### 3.3. The Coercivity Temperature Dependence of $\text{Mn}_{55}\text{Bi}_{45}/\text{Nd}_2\text{Fe}_{14}\text{B}$ Hybrid Magnetic Alloys

It was well-known that MnBi alloys characterized with a positive temperature coefficient of coercivity, and the coercivity increased constantly with the increase of temperature from 300 K to 400 K [24–26]. Therefore, in order to investigate the relationship between temperature and the coercivity of  $(\text{Mn}_{55}\text{Bi}_{45})_{100-x}/(\text{Nd}_2\text{Fe}_{14}\text{B})_x$  hybrid magnetic alloys, the magnetic properties at the temperatures from 300 K to 380 K were measured. Figure 5 showed the variation trends of the coercivity of  $(\text{Mn}_{55}\text{Bi}_{45})_{100-x}/(\text{Nd}_2\text{Fe}_{14}\text{B})_x$  hybrid magnetic alloys with the increase of temperature. For the pure  $\text{Mn}_{55}\text{Bi}_{45}$  ( $x = 0$ ), the coercivity enhanced significantly with the increase of temperature and reached 21.6 kOe at 380 K. However, with the increase of  $\text{Nd}_2\text{Fe}_{14}\text{B}$  content, the trend that coercivity increased with the increasing temperature declined gradually. For  $x = 20$ , LTP-MnBi was the dominant phase, so the coercivity increased with the increase of temperature, while the increasing trend was much weaker than that of pure  $\text{Mn}_{55}\text{Bi}_{45}$ . A coercivity of 17.7 kOe was obtained in  $(\text{Mn}_{55}\text{Bi}_{45})_{80}/(\text{Nd}_2\text{Fe}_{14}\text{B})_{20}$  hybrid magnetic alloy at 380 K. For  $x = 40$ , it was observed that the coercivity of  $(\text{Mn}_{55}\text{Bi}_{45})_{60}/(\text{Nd}_2\text{Fe}_{14}\text{B})_{40}$  hybrid magnetic alloy first increased and reached the maximum value of 16.2 kOe at 325 K but then began to decrease with the further increase of temperature. Furthermore, for  $x = 60$  and 80, the  $\text{Nd}_2\text{Fe}_{14}\text{B}$  phase, which featured with a negative temperature coefficient of coercivity, gradually became the dominant phase. Thus, the coercivity decreased with the increase of temperature. The relatively low coercivities of 14.1 kOe and 13.5 kOe were obtained in  $(\text{Mn}_{55}\text{Bi}_{45})_{40}/(\text{Nd}_2\text{Fe}_{14}\text{B})_{60}$  and  $(\text{Mn}_{55}\text{Bi}_{45})_{20}/(\text{Nd}_2\text{Fe}_{14}\text{B})_{80}$  hybrid magnetic alloys at 380 K.

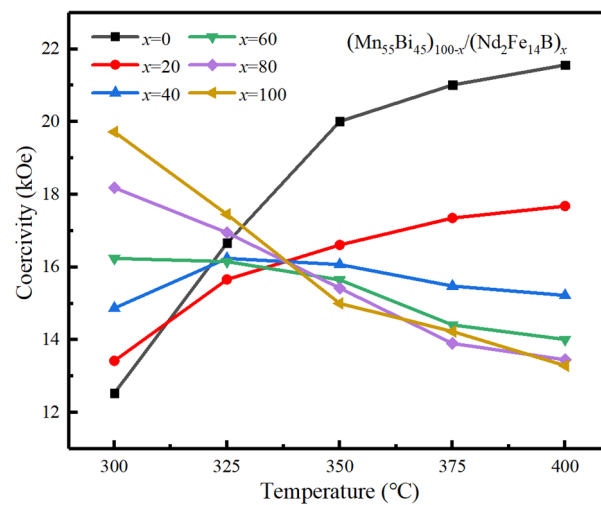


**Figure 5.** The temperature dependence of coercivity of the bulk  $(\text{Mn}_{55}\text{Bi}_{45})_{100-x}/(\text{Nd}_2\text{Fe}_{14}\text{B})_x$  ( $x = 0, 20, 40, 60, 80,$  and  $100$ ) hybrid magnetic alloys.

To further investigate the temperature characteristic of coercivity of the hybrid magnetic alloys, the temperature coefficient of coercivity  $K$  (Oe/K) was calculated by following formula:

$$K = \frac{H_{cT_2} - H_{cT_1}}{T_2 - T_1} \quad (1)$$

where  $T_1$  and  $T_2$  are the initial temperature and the final temperature and  $H_{cT_1}$  and  $H_{cT_2}$  are the coercivities at corresponding temperatures. The results were shown in Figure 6. The temperature coefficients of coercivity were calculated to be 78 Oe/K, 46 Oe/K, 3 Oe/K,  $-29$  Oe/K,  $-60$  Oe/K, and  $-78$  Oe/K for  $x = 0, 20, 40, 60, 80,$  and  $100$ , respectively. It was demonstrated that although the temperature coefficients of coercivity for  $(\text{Mn}_{55}\text{Bi}_{45})_{40}/(\text{Nd}_2\text{Fe}_{14}\text{B})_{60}$  and  $(\text{Mn}_{55}\text{Bi}_{45})_{20}/(\text{Nd}_2\text{Fe}_{14}\text{B})_{80}$  were still negative, they have been improved greatly compared to pure  $\text{Nd}_2\text{Fe}_{14}\text{B}$ . For  $(\text{Mn}_{55}\text{Bi}_{45})_{60}/(\text{Nd}_2\text{Fe}_{14}\text{B})_{40}$  and  $(\text{Mn}_{55}\text{Bi}_{45})_{80}/(\text{Nd}_2\text{Fe}_{14}\text{B})_{20}$ , the positive temperature coefficients of coercivity indicated good stability at high temperature. Therefore, the existence of the MnBi alloy can improve the high temperature magnetic properties of NdFeB alloy.

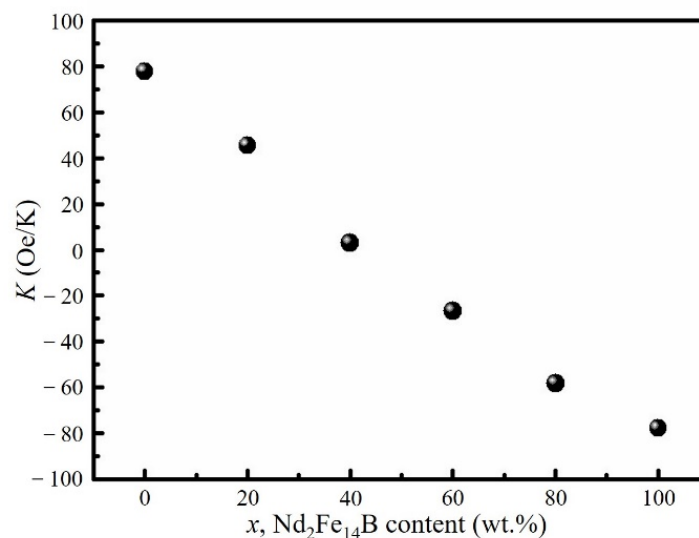


**Figure 6.** The temperature coefficient of coercivity of the bulk  $(\text{Mn}_{55}\text{Bi}_{45})_{100-x}/(\text{Nd}_2\text{Fe}_{14}\text{B})_x$  ( $x = 0, 20, 40, 60, 80,$  and  $100$ ) hybrid magnetic alloys.

### 3.4. The High Temperature Magnetic Properties of $\text{Mn}_{55}\text{Bi}_{45}/\text{Nd}_2\text{Fe}_{14}\text{B}$ Hybrid Magnetic Alloys

The magnetic properties of  $(\text{Mn}_{55}\text{Bi}_{45})_{100-x}/(\text{Nd}_2\text{Fe}_{14}\text{B})_x$  hybrid magnetic alloys at 350 K (the upper working temperature of  $\text{NdFeB}$  alloy) were investigated. As shown in Figures 7 and 8, and Table 3, the  $M_s$  for pure  $\text{Mn}_{55}\text{Bi}_{45}$  and pure  $\text{Nd}_2\text{Fe}_{14}\text{B}$  were measured to be 58.4 emu/g to 113.6 emu/g at 350 K, respectively. With the increase of  $\text{Nd}_2\text{Fe}_{14}\text{B}$  content from 20 wt.% to 80 wt.%, the  $M_s$  gradually increased, which was similar to the variation tendency at room temperature. However, the coercivity decreased gradually. For the pure  $\text{Mn}_{55}\text{Bi}_{45}$ , the highest  $H_c$  of 20.1 kOe was obtained, which was due to its positive temperature coefficient of coercivity. For  $(\text{Mn}_{55}\text{Bi}_{45})_{100-x}/(\text{Nd}_2\text{Fe}_{14}\text{B})_x$ , the  $H_c$  decreased to 16.6 kOe, 16.1 kOe, 15.6 kOe, and 15.4 kOe with  $\text{Nd}_2\text{Fe}_{14}\text{B}$  content of 20 wt.%, 40 wt.%, 60 wt.%, and 80 wt.%, respectively. The pure  $\text{Nd}_x\text{Fe}_{14}\text{B}$  exhibited the lowest  $H_c$  of 15.1 kOe. It was noteworthy that although the  $H_c$  gradually decreased with the increase of  $\text{Nd}_2\text{Fe}_{14}\text{B}$  content, the  $H_c$  (16.6 kOe and 16.1 kOe) of  $(\text{Mn}_{55}\text{Bi}_{45})_{80}/(\text{Nd}_2\text{Fe}_{14}\text{B})_{20}$  and  $(\text{Mn}_{55}\text{Bi}_{45})_{60}/(\text{Nd}_2\text{Fe}_{14}\text{B})_{40}$  at 350 K were higher than those (13.4 kOe and 14.8 kOe) at room temperature. Therefore, it was indicated that mixing with the  $\text{Mn}_{55}\text{Bi}_{45}$  alloy increased the coercivity of  $\text{Nd}_2\text{Fe}_{14}\text{B}$  alloy at 350 K, which indicated an enhanced anti-ferromagnetic ability. Furthermore, the  $(BH)_{\max}$  of 10.5 MGOe and 10.1 MGOe at 350 K were obtained in  $(\text{Mn}_{55}\text{Bi}_{45})_{40}/(\text{Nd}_2\text{Fe}_{14}\text{B})_{60}$  and  $(\text{Mn}_{55}\text{Bi}_{45})_{20}/(\text{Nd}_2\text{Fe}_{14}\text{B})_{80}$ , which was favorable for the applications at high temperature.

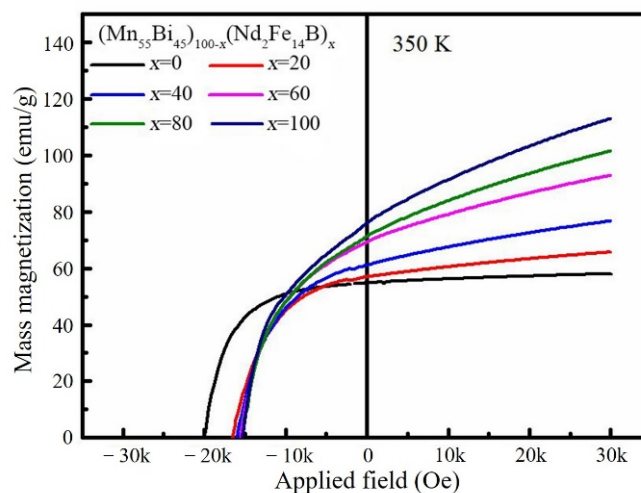


**Figure 7.** The demagnetization curves of the bulk  $(\text{Mn}_{55}\text{Bi}_{45})_{100-x}/(\text{Nd}_2\text{Fe}_{14}\text{B})_x$  ( $x = 0, 20, 40, 60, 80,$  and  $100$ ) hybrid magnetic alloys at 350 K.

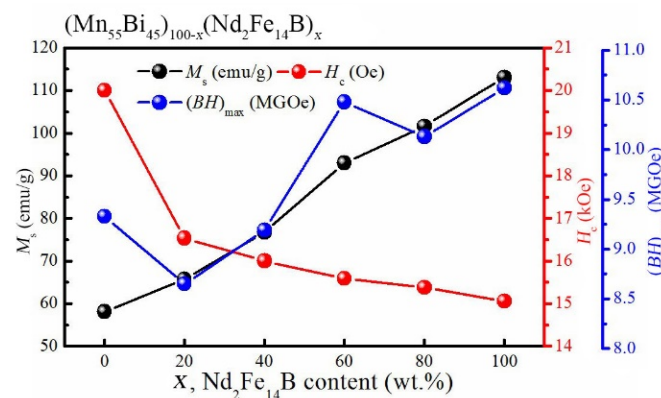


**Figure 8.** The variation curves of saturation magnetization ( $M_s$ ), coercivity ( $H_c$ ) and maximum energy product  $(BH)_{\max}$  of the bulk  $(\text{Mn}_{55}\text{Bi}_{45})_{100-x}/(\text{Nd}_2\text{Fe}_{14}\text{B})_x$  ( $x = 0, 20, 40, 60, 80,$  and  $100$ ) hybrid magnetic alloys at 350 K with the increase of  $\text{Nd}_2\text{Fe}_{14}\text{B}$  content.

**Table 3.** The magnetic properties of the bulk  $(\text{Mn}_{55}\text{Bi}_{45})_{100-x}/(\text{Nd}_2\text{Fe}_{14}\text{B})_x$  hybrid magnetic alloys at 350 K.

$(\text{Mn}_{55}\text{Bi}_{45})_{100-x}/(\text{Nd}_2\text{Fe}_{14}\text{B})_x$	$M_s$ (emu/g)	$H_c$ (kOe)	$(BH)_{\max}$ (MGOe)
$x = 0$	58.3 (8)	20.1 (2)	9.3 (5)
$x = 20$	66.2 (3)	16.6 (1)	8.5 (8)
$x = 40$	76.1 (6)	16.0 (9)	9.1 (8)
$x = 60$	92.9 (4)	15.6 (4)	10.4 (9)
$x = 80$	101.7 (2)	15.4 (3)	10.1 (3)
$x = 100$	113.6 (3)	15.1 (1)	10.6 (2)

#### 4. Conclusions

The bulk  $(\text{Mn}_{55}\text{Bi}_{45})_{100-x}/(\text{Nd}_2\text{Fe}_{14}\text{B})_x$  ( $x = 0, 20, 40, 60, 80,$  and  $100$ ) hybrid magnetic alloys were successfully prepared by following processes: induction melting, vacuum annealing, ball milling, and cold press. The magnetic properties at the temperatures from 300 K to 380 K were investigated. With the increase of  $\text{Nd}_2\text{Fe}_{14}\text{B}$  content, both the saturation magnetization and coercivity of the hybrid magnetic alloys at room temperature were increased compared to the pure  $\text{Mn}_{55}\text{Bi}_{45}$ . The increased energy products of 10.8 MGOe and 11.5 MGOe were obtained in  $(\text{Mn}_{55}\text{Bi}_{45})_{40}/(\text{Nd}_2\text{Fe}_{14}\text{B})_{60}$  and  $(\text{Mn}_{55}\text{Bi}_{45})_{20}/(\text{Nd}_2\text{Fe}_{14}\text{B})_{80}$ , respectively, which were 10% and 17% higher than those in pure  $\text{Mn}_{55}\text{Bi}_{45}$ . At elevated temperatures, due to the positive temperature coefficient of the coercivity of MnBi alloy, the hybrid magnetic alloys exhibited good magnetic properties. The coercivities of 16.6 kOe and 16.1 kOe were obtained in  $(\text{Mn}_{55}\text{Bi}_{45})_{80}/(\text{Nd}_2\text{Fe}_{14}\text{B})_{20}$  and  $(\text{Mn}_{55}\text{Bi}_{45})_{60}/(\text{Nd}_2\text{Fe}_{14}\text{B})_{40}$  at 350 K, which indicated a 24% increase and a 9% increase compared to those at room temperature. An energy product of 10.5 MGOe was obtained in  $(\text{Mn}_{55}\text{Bi}_{45})_{40}/(\text{Nd}_2\text{Fe}_{14}\text{B})_{60}$  at 350 K. It was demonstrated that  $(\text{Mn}_{55}\text{Bi}_{45})_{100-x}/(\text{Nd}_2\text{Fe}_{14}\text{B})_x$  hybrid magnetic alloys can exhibit good magnetic properties at room temperature and high temperature, which is favorable for its application in various fields.

**Author Contributions:** Conceptualization, Z.X. and S.L.; methodology, Y.Y.; Resources, Y.Y.; software, L.C. and S.L.; formal analysis, L.C.; investigation, S.L.; data curation, Z.X.; writing—original draft preparation, S.L.; writing—review and editing, W.L.; visualization, L.C.; supervision, Z.X.; project administration, Z.X.; funding acquisition, W.L. All authors have read and agreed to the published version of the manuscript.

**Funding:** This work was supported by the National Key Research and Development Program of China (Grant No. 2019YFE0122900), the National Natural Science Foundation of China (Grant No. 52101229, 51971162 and U1933112), and the China Postdoctoral Science Foundation (Grant No. 2020M671208).

**Data Availability Statement:** Not applicable.

**Conflicts of Interest:** The authors declare no conflict of interest.

#### References

1. Coey, J.M.D. Perspective and Prospects for Rare Earth Permanent Magnets. *Engineering* **2020**, *6*, 119–131. [[CrossRef](#)]
2. McCallum, R.W.; Lewis, L.; Skomski, R.; Kramer, M.J.; Anderson, I.E. Practical Aspects of Modern and Future Permanent Magnets. *Annu. Rev. Mater. Res.* **2014**, *44*, 451–477. [[CrossRef](#)]
3. Coey, J.M. New permanent magnets; manganese compounds. *J. Phys. Condens. Matter.* **2014**, *26*, 064211. [[CrossRef](#)] [[PubMed](#)]
4. Sarkar, A.; Mallick, A.B. Synthesizing the Hard Magnetic Low-Temperature Phase of MnBi Alloy: Challenges and Prospects. *Jom* **2020**, *72*, 2812–2825. [[CrossRef](#)]
5. Cui, J.; Kramer, M.; Zhou, L.; Liu, F.; Gabay, A.; Hadjipanayis, G.; Balasubramanian, B.; Sellmyer, D. Current progress and future challenges in rare-earth-free permanent magnets. *Acta Mater.* **2018**, *158*, 118–137. [[CrossRef](#)]
6. Cui, J.; Choi, J.-P.; Polikarpov, E.; Bowden, M.E.; Xie, W.; Li, G.; Nie, Z.; Zarkevich, N.; Kramer, M.J.; Johnson, D. Effect of composition and heat treatment on MnBi magnetic materials. *Acta Mater.* **2014**, *79*, 374–381. [[CrossRef](#)]
7. Park, J.; Hong, Y.-K.; Lee, J.; Lee, W.; Kim, S.-G.; Choi, C.-J. Electronic Structure and Maximum Energy Product of MnBi. *Metals* **2014**, *4*, 455–464. [[CrossRef](#)]
8. Patel, K.; Zhang, J.; Ren, S. Rare-earth-free high energy product manganese-based magnetic materials. *Nanoscale* **2018**, *10*, 11701–11718. [[CrossRef](#)]

9. Yang, J.; Yang, W.; Shao, Z.; Liang, D.; Zhao, H.; Xia, Y.; Yang, Y. Mn-based permanent magnets. *Chin. Phys. B* **2018**, *27*, 117503. [[CrossRef](#)]
10. Yang, Y.; Park, J.; Lim, J.T.; Kim, J.-W.; Li, O.L.; Choi, C.-J. Effect of phase purity on enhancing the magnetic properties of Mn-Bi alloy. *J. Magn. Magn. Mater.* **2021**, *517*, 167344. [[CrossRef](#)]
11. Xiang, Z.; Wang, T.; Ma, S.; Qian, L.; Luo, Z.; Song, Y.; Yang, H.; Lu, W. Microstructural evolution and phase transformation kinetics of MnBi alloys. *J. Alloys Compd.* **2018**, *741*, 951–956. [[CrossRef](#)]
12. Cui, J.; Choi, J.P.; Li, G.; Polikarpov, E.; Darsell, J.; Overman, N.; Olszta, M.; Schreiber, D.; Bowden, M.; Droubay, T. Thermal stability of MnBi magnetic materials. *J. Phys. Condens. Mat.* **2014**, *26*, 064212. [[CrossRef](#)]
13. Gabay, A.M.; Hadjipanayis, G.C.; Cui, J. Preparation of highly pure  $\alpha$ -MnBi phase via melt-spinning. *AIP Adv.* **2018**, *8*, 056702. [[CrossRef](#)]
14. Xiang, Z.; Song, Y.; Pan, D.; Shen, Y.; Qian, L.; Luo, Z.; Liu, Y.; Yang, H.; Yan, H.; Lu, W. Coercivity enhancement and magnetization process in Mn55Bi45 alloys with refined particle size. *J. Alloys Compd.* **2018**, *744*, 432–437. [[CrossRef](#)]
15. Xiang, Z.; Xu, C.; Wang, T.; Song, Y.; Yang, H.; Lu, W. Enhanced magnetization and energy product in isotropic nanocrystalline Mn55Al45 alloys with boron doping. *Intermetallics* **2018**, *101*, 13–17. [[CrossRef](#)]
16. Gabay, A.M.; Hadjipanayis, G.C.; Cui, J. New anisotropic MnBi permanent magnets by field-annealing of compacted melt-spun alloys modified with Mg and Sb. *J. Magn. Magn. Mater.* **2020**, *495*, 165860. [[CrossRef](#)]
17. Xiang, Z.; Song, Y.; Deng, B.; Cui, E.; Yu, L.; Lu, W. Enhanced formation and improved thermal stability of ferromagnetic  $\tau$  phase in nanocrystalline Mn55Al45 alloys by Co addition. *J. Alloys Compd.* **2019**, *783*, 416–422. [[CrossRef](#)]
18. Yang, J.B.; Yang, Y.B.; Chen, X.G.; Ma, X.B.; Han, J.Z.; Yang, Y.C.; Guo, S.; Yan, A.R.; Huang, Q.Z.; Wu, M.M.; et al. Anisotropic nanocrystalline MnBi with high coercivity at high temperature. *Appl. Phys. Lett.* **2011**, *99*, 082505. [[CrossRef](#)]
19. Yang, Y.; Kim, J.-W.; Si, P.-Z.; Qian, H.-D.; Shin, Y.; Wang, X.; Park, J.; Li, O.L.; Wu, Q.; Ge, H.; et al. Effects of Ga-doping on the microstructure and magnetic properties of MnBi alloys. *J. Alloys Compd.* **2018**, *769*, 813–816. [[CrossRef](#)]
20. Bae, C.; Lee, G.; Kang, M.K.; Lee, H.; Moon, K.W.; Kim, J. Synthesis and Magnetic Properties of Sb added MnBi Magnets for Applications at Sub-zero Temperatures. *J. Alloys Compd.* **2021**, *899*, 163365. [[CrossRef](#)]
21. Xu, X.; Hong, Y.-K.; Park, J.; Lee, W.; Lane, A.M.; Cui, J. Magnetic self-assembly for the synthesis of magnetically exchange coupled MnBi/Fe–Co composites. *J. Solid. State. Chem.* **2015**, *231*, 108–113. [[CrossRef](#)]
22. Yang, Y.B.; Wei, J.Z.; Peng, X.L.; Xia, Y.H.; Chen, X.G.; Wu, R.; Du, H.L.; Han, J.Z.; Wang, C.S.; Yang, Y.C.; et al. Magnetic properties of the anisotropic MnBi/Sm2Fe17Nx hybrid magnet. *J. Appl. Phys.* **2014**, *115*, 17A721. [[CrossRef](#)]
23. Akiya, T.; Kato, H.; Sagawa, M.; Koyama, K. Enhancement of coercivity in Al and Cu added Nd-Fe-B sintered magnets by high field annealing. *IOP Conf. Ser. Mater. Sci. Eng.* **2009**, *1*, 012034. [[CrossRef](#)]
24. Yang, J.B.; Yelon, W.B.; James, W.J.; Cai, Q.; Roy, S.; Ali, N. Structure and magnetic properties of the MnBi low temperature phase. *J. Appl. Phys.* **2002**, *91*, 7866–7868. [[CrossRef](#)]
25. Yang, J.B.; Kamaraju, K.; Yelon, W.B.; James, W.J.; Cai, Q.; Bollero, A. Magnetic properties of the MnBi intermetallic compound. *Appl. Phys. Lett.* **2001**, *79*, 1846–1848. [[CrossRef](#)]
26. Song, Y.; Xiang, Z.; Wang, T.; Niu, J.; Xia, K.; Lu, W.; Zhang, H.; Cao, Y.; Yoshimura, S.; Saito, H. High temperature exchange bias effect in melt-spun Mn55Bi45alloys. *Appl. Phys. Lett.* **2016**, *109*, 112402. [[CrossRef](#)]